DOI: 10.5604/01.3001.0016.0941
Volume 113 • Issue 1 • July 2022
Journal of Achievements in Materials and Manufacturing Engineering
International Scientific Journal published monthly by the World Academy of Materials and Manufacturing Engineering

FEM numerical simulation of contact stresses between driving shaft and hub impeller of fuel pump

M. Wiater [a,b,*], G. Chladek [b], J. Żmudzki [b]
[a] TI Poland Sp. z o.o., ul. Bestwińska 143a, 43-346 Bielsko-Biała, Poland
[b] Chair of Engineering Materials and Biomaterials, Faculty of Mechanical Engineering, Silesian University of Technology, ul. Konarskiego 18a, Gliwice 44-100, Poland
* Corresponding e-mail address: maciej.wiater@polsl.pl
ORCID identifier: https://orcid.org/0000-0001-8282-4131 (G.C.);
https://orcid.org/0000-0003-1044-2358 (J.Ż.)

ABSTRACT

Purpose: The aim of the work was to test the contact stresses in the model system of the turbine hub cooperating with the fuel pump drive shaft. The hypothesis of the work was that, by means of FEA, it is possible to assess the contact stresses in the materials of the turbine hub and the fuel pump shaft during torque transmission.

Design/methodology/approach: A turbine with fibre-reinforced polyphenylene sulphide (PPS) composite cooperating with a stainless steel shaft (X46Cr13/1.4034) in a commonly used D-flat shape joint was selected for the experimental research. To assess contact stresses, the CAD model (NX, Siemens) of the entire turbine was limited to the hub area. The drive shaft is supported in accordance with the bearing in the fuel pump, and the possibility of rotation about the axis along the length of the torque-producing magnet is taken away. The system was loaded with a torque of 200 Nmm on the turbine. The turbine hub and shaft were calculated, taking into account the phenomenon of contact detachment or slip at the value of the friction coefficient of 0.1.

Findings: The pressure transmission area was found in the area at the edge of the flat surface D-flat and on the opposite side of the D-convexity. The contact stresses on the D-flat side reached values close to the composite strength.

Research limitations/implications: The studies did not take into account the technological inaccuracies, thermal deformation, local material properties, and wear. The value of the friction coefficient was not measured in realistic conditions with fuel lubrication.

Practical implications: FEA has been achieved, which allows to reduce the cost of experimental research.

Originality/value: The proposed model allows for further studies of the influence of elasticity of various materials and structures on contact stresses in order to assess wear resistance.

Keywords: Fibre reinforcement composite, Fuel pump, Impeller, Shaft, Hub wear, Contact stress, Finite Elements Analysis (FEA)

Reference to this paper should be given in the following way:
M. Wiater, G. Chladek, J. Żmudzki, FEM numerical simulation of contact stresses between driving shaft and hub impeller of fuel pump, Journal of Achievements in Materials and Manufacturing Engineering 113/1 (2022) 13-21. DOI: https://doi.org/10.5604/01.3001.0016.0941

ANALYSIS AND MODELLING

1. Introduction

The materials and technologies that worked excellently in the past decades of automotive production also met the requirements of both manufacturers and their end users [1,2]. Much of the fuel system components, especially the fuel pumps feeding the fuel systems, were designed at the end of the last century. However, the continuous increase in requirements for car manufacturers with regard to the performance of vehicles, their internal combustion engines, meeting increasingly restrictive ecological standards, reducing exhaust emissions and fuel consumption, as well as introducing hybrid systems resulted in a sharp change in environmental conditions and operating parameters, as well as a continuous increase in material loads of the fuel system components. There is a need to adapt the system components combined with more modern elements increasing their efficiency, and improving the possibility of their precise control while adapting them to the constantly growing requirements of hybrid technology.

Over the last several years, there has been an increase in the fuel pressure in the fuel systems from about 3.5-4.0 bar to about 6.0-7.5 bar. Bio-components have been introduced in fuels, which have an increasing impact on changes in the functional properties and degradation of the materials used to build many of the elements of the fuel system. The need to cool other components with flowing fuel, as well as increased engine work parameters, resulted in an increase in operating temperature. The original material selection criteria were adapted to the characteristics of the relatively weak DC motors, which have now been replaced by electronically commutated (BLDC) drive systems that generate much higher torques. Start-stop systems and systems turning off the fuel system pumps while the hybrid vehicle is moving have appeared, increasing the number of system starts and stop cycles, as well as sudden loads on the pressure-building elements.

One of the systems that, due to the risk of a decrease in reliability, requires verification of the selection of materials and technologies is the form-fit connection of the fuel pump turbine with the shaft. Shaping the functional properties of cooperating materials in a fitted connection of a structural node requires verification of the increased load transfer by simulation tests of the stress state [3,4]. The evaluation criterion is the state of contact stresses in the joint and the entire element since the local improvement of the wear resistance may not lead to a critical reduction of strength outside the area of the sliding joint. Depending on the factors mentioned above, verification of the state of stress is the starting point for further analyses and selection of materials.

The aim of the work was to propose a numerical model of the FEM, which allows for the study of contact stresses in the turbine hub system cooperating with the fuel pump drive shaft. The hypothesis of the work was that, by means of FEA, it is possible to assess the contact stresses in the materials of the turbine hub and the fuel pump shaft during torque transmission

2. Methodology

Geometric CAD shaft and fuel impeller models were imported to Nx CAD (Siemens PLM) – Figure 1. Experimental modifications – roundings were introduced at the edges of the D-flat plane of the D-drive coupling (Fig. 2).

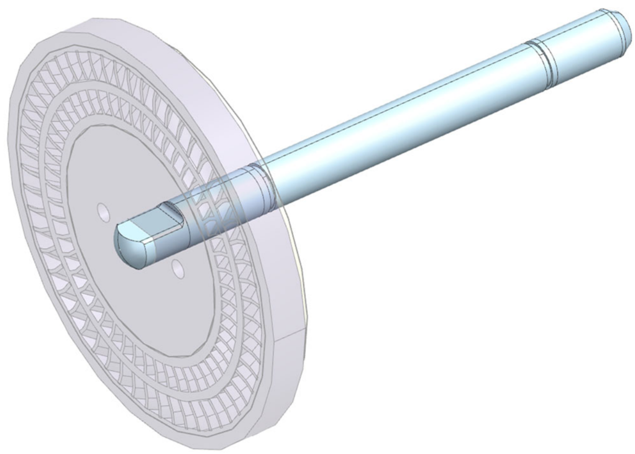

Fig. 1. Shaft and impeller CAD models

The FEM model was limited by cutting the inner part of the turbine in the hub area (Fig. 3) in order to reduce the size and computational effort of the FEA.

The shaft was made of stainless steel 1.4034 (X46Cr13) with a modulus of elasticity 200 GPa, and the impeller of short fiberglass reinforcement polifenylenosulfide composite (FG/PPS) with 3 GPa and both materials had Poisson ratio about of 0.3. The model was loaded with 200 Nmm torque at the impeller and circumferentially constrained at the shaft; hence resistance from fuel flow at the impeller and driving force were changed; reaction and driving moment were inverted in the calculation. Displacement constraints were added at the slide-bearing surface in the radial direction, on the shaft in the circumferential direction and at the shaft end in the axial direction.

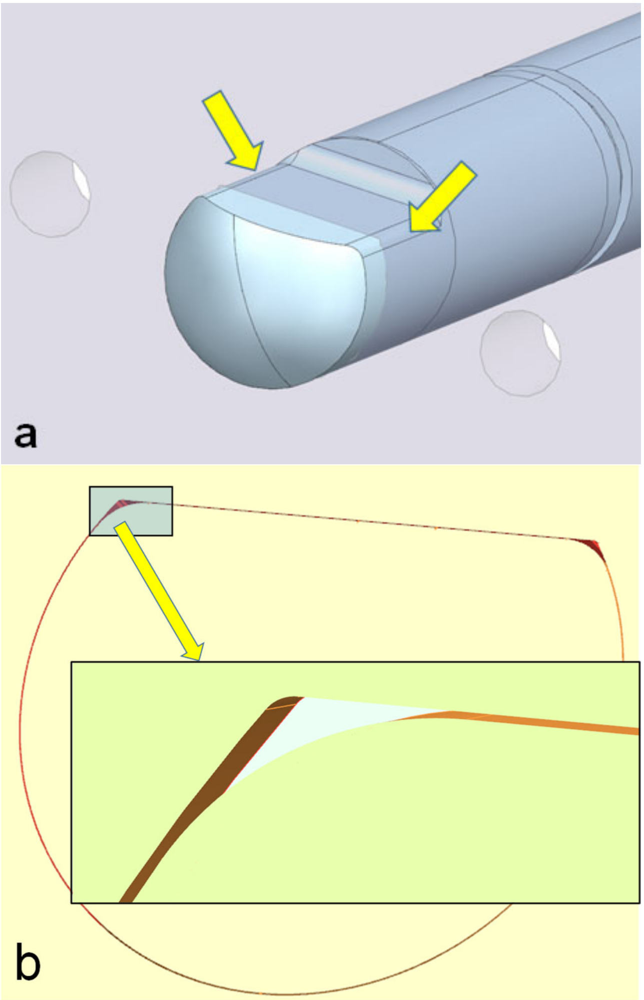

Fig. 2. Shaft and impeller fillets at edges in D-drive coupling

Between the shaft and the hub of the impeller contact was established with a value of friction coefficient of 0.1. Surface to surface and the Augmented Lagrangian method were used for contact calculation and contact pressure. The model size was 27 650 elements (45308 nodes) for the initially tested mesh with tetragonal 10-node elements – Figure 4.

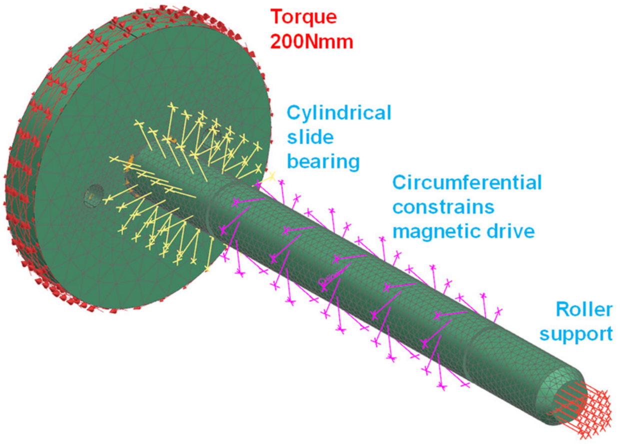

Fig. 3. Finite element model with boundary conditions: displacements constrained at slide bearing surface in the radial direction, on the shaft in the circumferential direction, at the shaft end in the axial direction and torque loading assumed at the inner surface to decrease the size of analysis

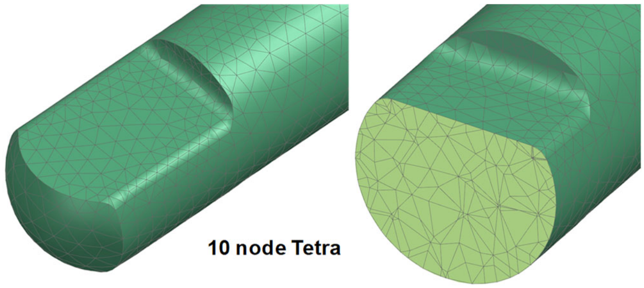

Fig. 4. Initially tested mesh with tetragonal 10-node elements

Then, for greater accuracy, contact surfaces were divided with high quality hexagonal 20-node second-order elements. The "boundary layer" mesh control option was used, and three hex element layers with 0.1 mm size and 0.9 growth rate parameter (Fig. 5). The model has reached the size 220 000 partially composed of hex elements according to the specification – Table 1.

Table 1.
Model specification

Total number of elements in part	219948
Total number of nodes in part	399476
Number of Quad4 elements	10532
Number of Tri3 elements	4
Number of Tetra10 elements	167516
Number of Hex20 elements	30162
Number of Pyr13 elements	11734

Calculation time was 4-8 h depending on number of elements (AMD Ryzen 7 2700 Eight-Core Processor 3.20 GHz and 16 GB RAM) with enabling of parallel computing.

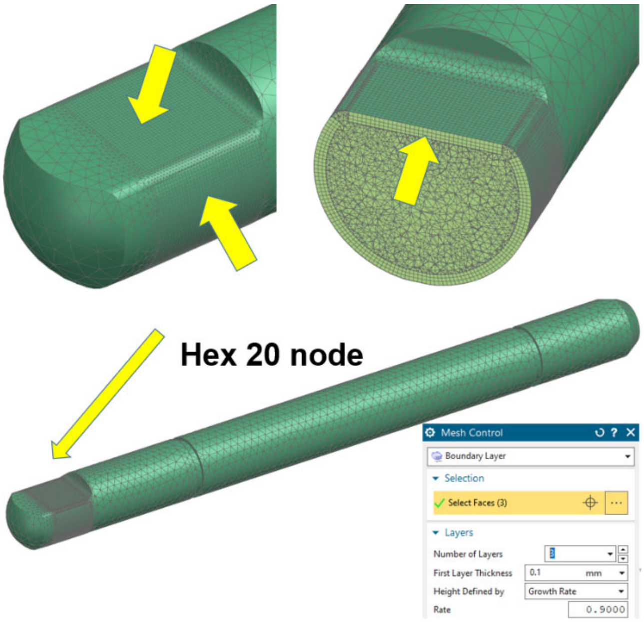

Fig. 5. Contact surfaces meshing with hexahedral 20-node parabolic elements with the use "boundary layer" mesh control

3. Results

3.1. Stress distribution

Based on the equivalent Huber-Mises stress in Figure 6, the influence of elements and the mesh quality is visible in the achieved results. The stress distribution is rather coarse in spite of enabling the averaging node values in the case of initially tested mesh with 10-tetra elements. The smooth stress distribution is achieved in the case of the use of 20-node hexahedral elements. The sectional view shows that the stress from the torsion is not greater than 30 MPa around the groove which is not a dangerous value for the steel. The highest stress value was observed from compression into the coupling with the impeller. Stress in the impeller was caused by compression in the D-drive joint – Figure 7 and Figure 8. The torque caused stresses at the D-flat edge and on the bulges. The depth of the higher stress zone was greater at the edge, and the value of 30-50 MPa reached 0.3-0.5 mm. Nodal and elemental minimal principal stress value comparison in Figure 8 shows that mesh quality was quite good to conclude that at a depth beyond the first contacting finite elements, the stresses reached 50 MPa.

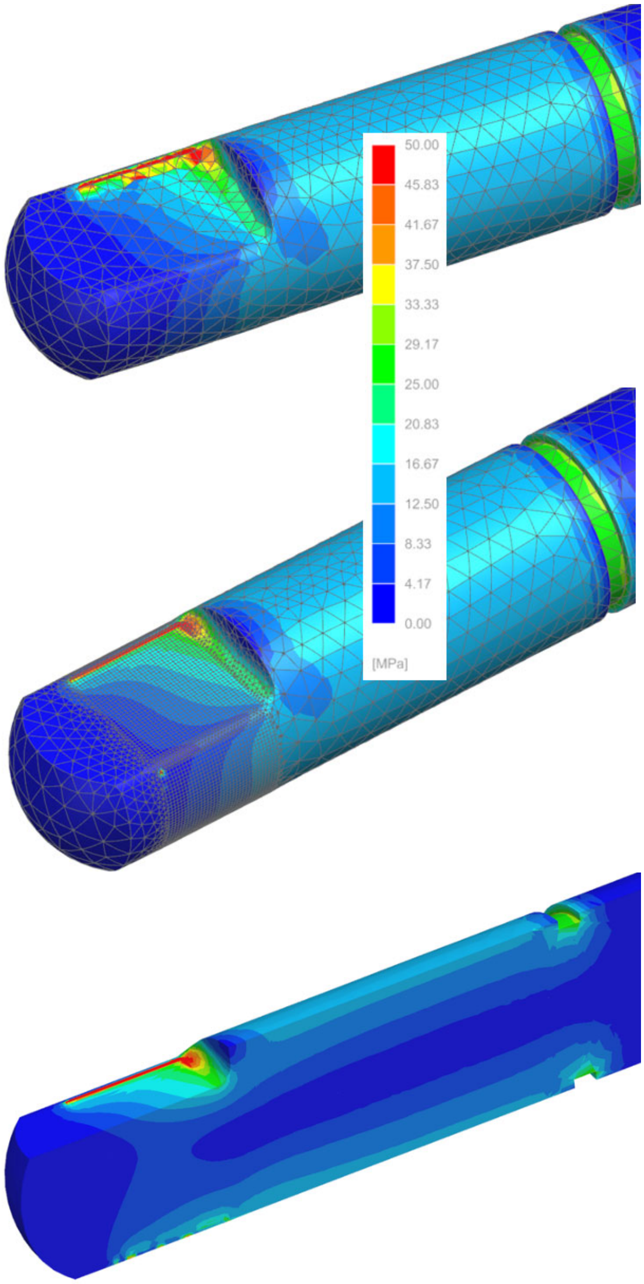

Fig. 6. Equivalent Huber-Mises stress in the shaft in the case of initial tested 10-node tetrahedral mesh and final mesh mixed with 20-node hexahedral elements

3.2. Contact stress

Contact pressure distribution and displacements into D-drive coupling and shaft were shown in Figure 9 and Figure 10. It was smooth in assumed finite element mesh resolution of about 0.1mm and agreement with compression stress.

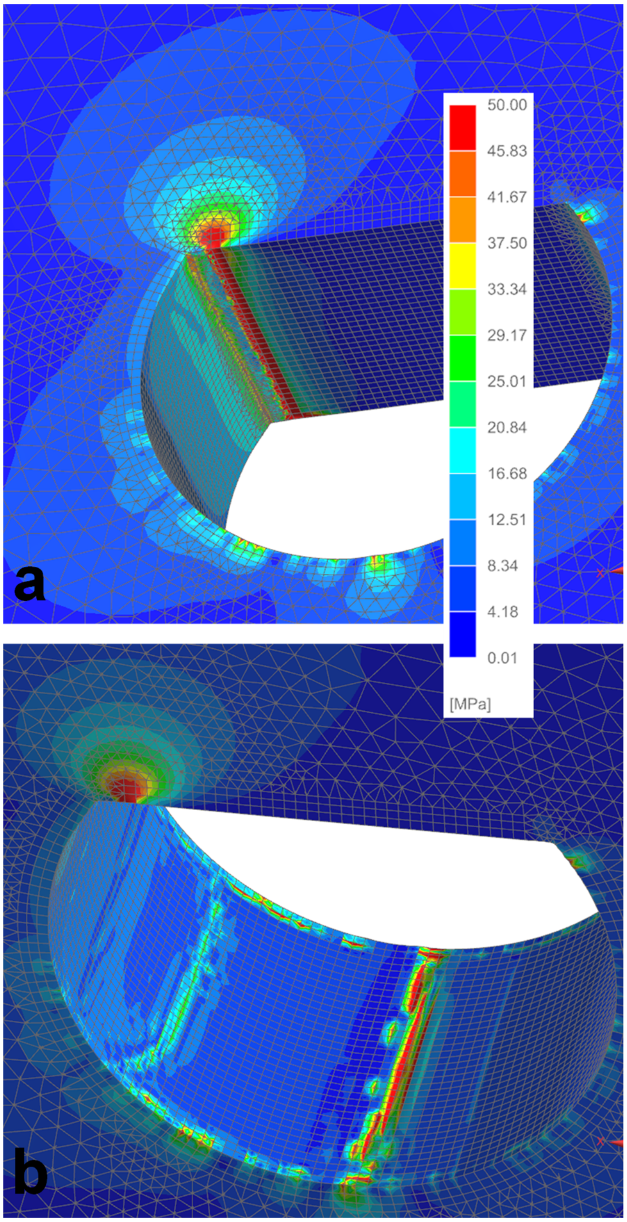

Fig. 7. Equivalent Huber-Mises stress in the FG/PPS impeller in the case of final fine mesh: upper the D-flat plane (a) and bottom rounded surface (b)

It reached about 50 MPa at finite elements next to the first elements being in contact. In the first contacting elements, stress reached about 80 MPa value. The compression stress value was not critical for the steel, especially since it can reach hardness of about 54 HRC. The shaft strength is enough, and only friction wear can be considered for local inequalities and aggressive corrosion contents. These values are very dangerous for the composite impeller hub.

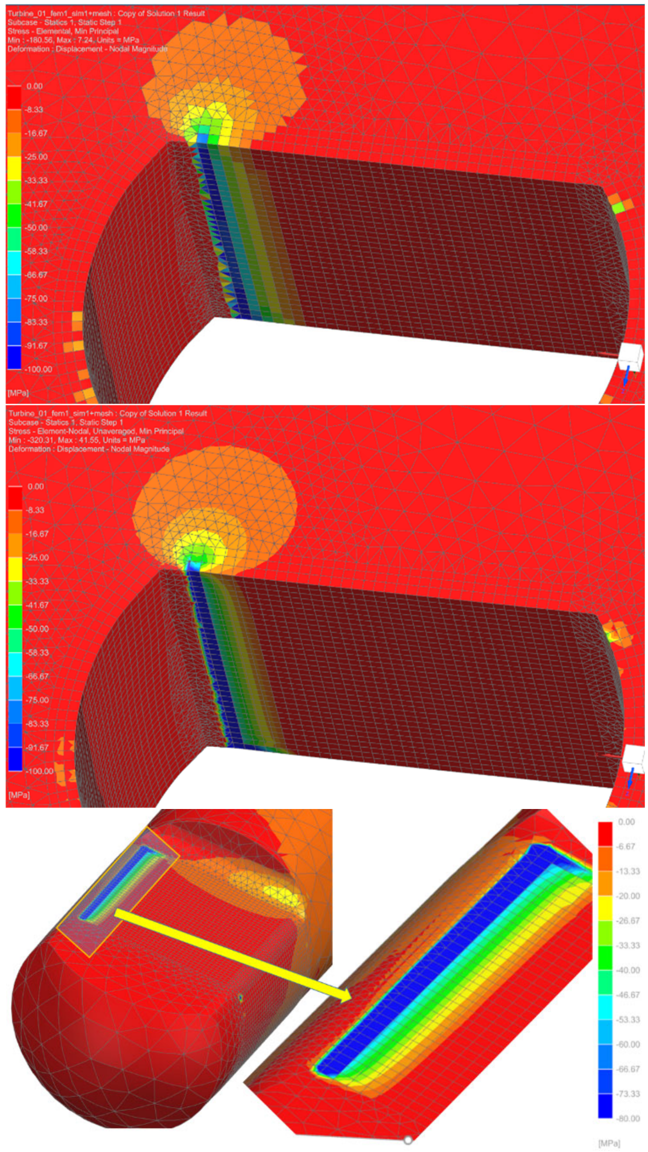

Fig. 8. Minimum principal stress comparison of elemental and nodal value and shaft D-flat plane nodal values

The value was near the PPS matrix strength. Especially when compared to the displacements that occur on the surface during friction and cause a risk of extensive wear. However, the next local model should be made to precisely calculate local contact pressure and compression.

4. Discussion

Many papers describe the failure mechanism and stress state using FEM modelling in keyed and splined shafts and hubs, including their wear, fretting, fatigue and fracture [3-9].

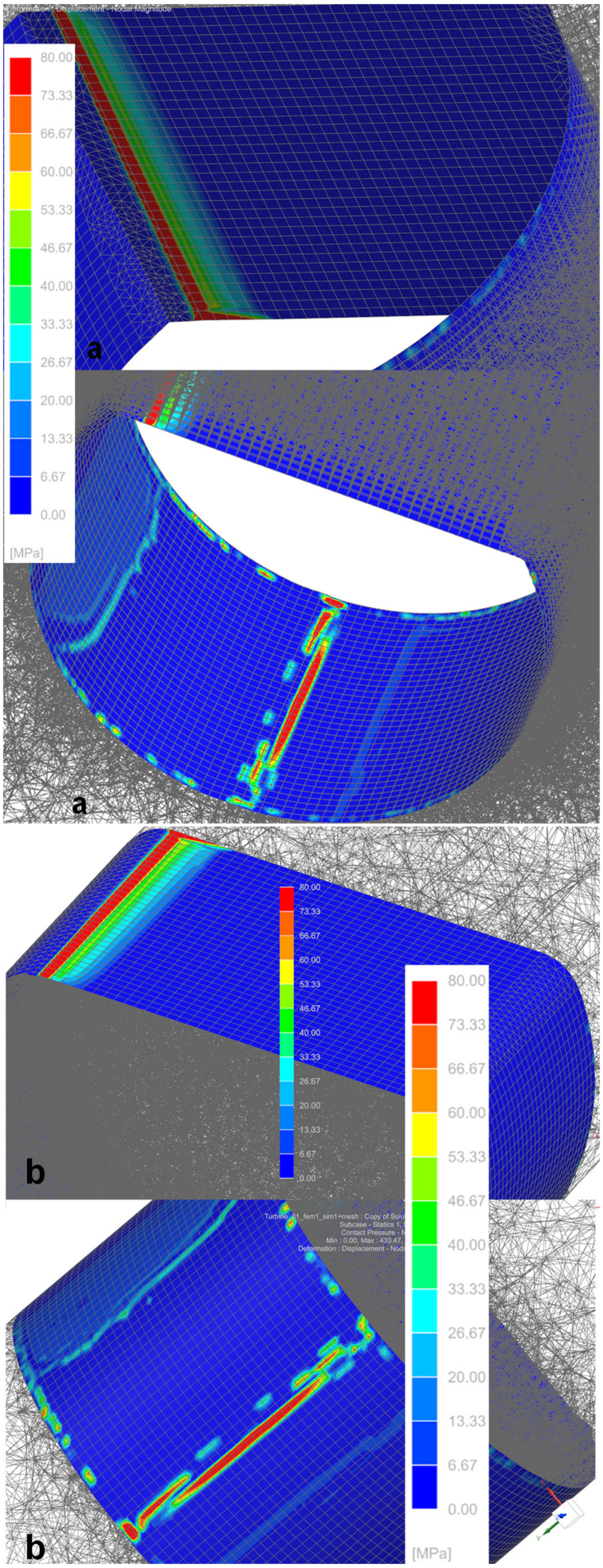

Fig. 9. Contact stress between impeller hub (a) and shaft (b)

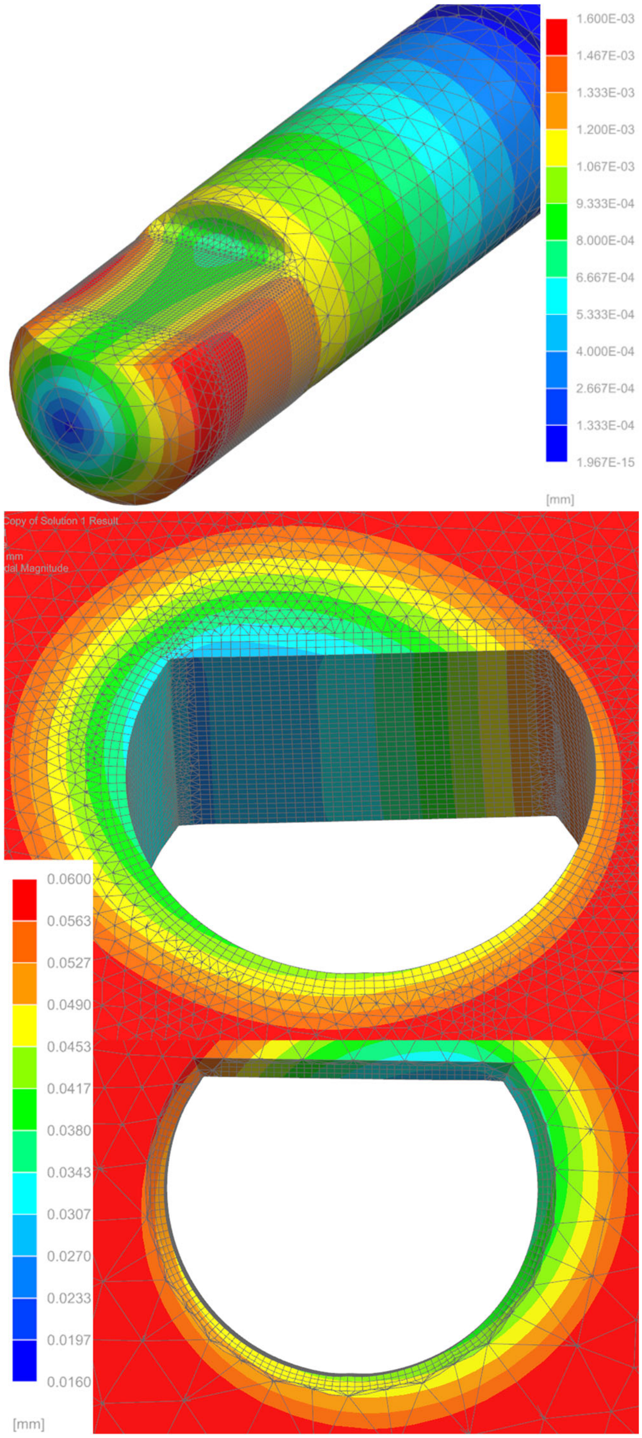

Fig. 10. Displacements of the shaft and into the D-drive coupling

There are known joint solutions with special shapes, which are designed to distribute the transferred forces over a larger area, reduce contact stress and wear, or reduce the impact of the notch [8,10]. Although these special connections are said to be clearance-free (press-fit) and with higher demand on component tolerances than standard connections [10,11], however, the uneven contact stress distribution makes this connection susceptible to failure under dynamic torsion load [12,13]. At the same time, in the case of mass production, the cost of shaft production is crucial, which is due to the shapes to be machined is relatively higher compared to the D-drive coupling.

Less is known about failure mechanisms in a D-drive connection, and the calculated stress values are difficult to compare as there are no similar models. Modelling the state of contact stresses is more difficult than the bending stresses of gear teeth [11]. Increasing the accuracy by increasing the number of finite elements in the criteria area significantly affects the effort of the calculations because the critical zone and the criteria values are in the area of nonlinear behaviour [14]. The mesh quality was tested in 3 sequences of the number of finite elements along the contact edge from several to about 40 (mesh size about 0.1 mm). High-quality hexahedral elements were generated along the edge of the contact and throughout its entire area as well as into the three layers. The quality of the mesh was better than, for example, in the works [15] and comparable to the works [9-19], in which the spline shaft finite element model was verified in experimental test by photo elasticity and analytical formula. The error value between FEM shear stress and the analytical solution was on the level of 3% and photo elasticity measurement in the range of 5-10%. In work [14] with a similar number of elements along the contact line of two deformable cylinders, the contact stress value calculated using analytical Hertz's formula does not differ by more than 8.7%, i.e. FEA shows a very good agreement. In the work [14] it was shown that the FEA of interference-fitted joints gives better results than traditional design on the basis of the analytical formulas [14,18].

Deformations in the system affect load sharing [11,17], therefore, the research took into account the shaft model with supports, although it is outside the criteria area and increases the cost of the analysis. Pure torsion loading transmitted in the D-drive connection and contact stresses show the difference compared to the symmetrical spline joints [4] as the load distribution in the D-drive is not symmetrical.

A hub made of fibre- and particle-reinforced composite, working in contact with steel in the event of being released from the matrix, may lead to various wear scenarios. The bare fibres of the damaged carcass act like a grinding wheel against the steel. However, the released reinforced particles will work as abrasive both against the shaft and hub before they are washed away.

Forecasting of wear processes with material loss is available, which allows us to take into account changes in the shape of an element after a specified period of operation. Shape changes lead to a new distribution of contact stresses. In the case of composite, such wear patterns are very complex. In the case of transferring contact stresses in composite materials, local heterogeneous material properties are stress concentrators (material notches). If the stress concentrations interfere with local concentrations of contact stresses, the expected reinforcement may not be obtained, or the matrix may be damaged, and the wear resistance deteriorated. In the process of wear, another parameter is the lubricating properties of the environment [20,21], which on the one hand, reduce wear when lubricating, but on the other hand, if the viscosity accumulates impurities, they can act as an abrasive.

An important element of the research is, therefore, to determine the stress state in the matrix on a micro-scale, which may lead to a micro-damage and gradual exposure of the applied reinforcement. In injection moulding, the distribution of the fibres is flow dependent and varies locally.

In engineering practice, the basis is to determine the division of stress distribution in the material and contact pressure, slip and stick-slip areas, which allow for the determination of friction work [22,23] depending on the shape and deformation of the cooperating elements of the structure. Cyclic stresses in crystalline polymers often lead to a reduction in the degree of crystallinity. On the one hand, this leads to a decrease in strength, but on the other hand, a high degree of crystallinity may result in brittleness against impact loads.

The impact of misalignment in the D-drive has not been known, while in spline couplings, it causes an increase in stress on the spline teeth, wear and fretting fatigue of splines [3,17]. The study assumed perfect geometry and ignored the influence of dimensional inaccuracies. Meanwhile, among spline teeth, some of them experience more damage than others, which is probably the result of a mismatch. Clearance and misalignment [16,17] set one of the directions for a further development of models and simulation research of the D-drive couplings wear.

5. Conclusions

Torque loading simulation into fuel pump D-drive coupling showed that the shaft and hub can experience wear at the edge of the flat surface, where also fatigue may occur in the glass fibre-reinforced PPS composite impeller hub.

References

[1] T. Tański, L.A. Dobrzański, M. Wiśniowski, T. Linek, R. Szklarek, PVD surface treatment of heat-treated cast aluminium alloys, Archives of Materials Science and Engineering 79/2 (2016) 79-88.
DOI: https://doi.org/10.5604/18972764.1229429

[2] T. Linek, T. Tański, W. Borek, Numerical analysis of the cavitation effect occurring on the surface of steel constructional elements, Archives of Materials Science and Engineering 85/1 (2017) 24-34.
DOI: https://doi.org/10.5604/01.3001.0010.1555

[3] H.W. Brown, A reliable spline coupling, Journal of Engineering for Industry 101/4 (1979) 421-426. DOI: https://doi.org/10.1115/1.3439531

[4] V. Kovan, Separation frequency analysis of interference fitted hollow shaft–hub connections by finite element method, Advances in Engineering Software 42/9 (2011) 644-648.
DOI: https://doi.org/10.1016/j.advengsoft.2011.05.001

[5] J. Hong, D. Talbot, A. Kahraman, Load Distribution Analysis of Spline Joints, Gear Technology May (2014) 44-48.

[6] L. Limmer, D. Nowell, D.A. Hills, A combined testing and modeling approach to the prediction of the fretting fatigue performance of splined shafts, Proceedings of the Institution of Mechanical Engineers, Part G: Journal of Aerospace Engineering 215/2 (2001) 105-112. DOI: https://doi.org/10.1243/0954410011531808

[7] Z. Kahn-Jetter, S. Wright, Finite Element Analysis of an Involute Spline, Journal of Mechanical Design 122/2 (2000) 239-244.
DOI: https://doi.org/10.1115/1.533573

[8] M. Ziaei, Analytical investigation of non-round profile families and numerical optimization of standardized polygon profiles for shaft-hub connections, Habilitation Thesis, TU Chemnitz, 2002 (in German).

[9] S.B. Patil, S.R. Patil, Experimental and numerical analysis of a load distribution along the length of contact in involute spline shaft, International Journal of Advanced Technology and Engineering Exploration 6/51 (2019) 30-44.
DOI: https://doi.org/10.19101/IJATEE.2019.650006

[10] D. Ulrich, H. Binz, An enhanced design method for 3D contact surfaces on shaft–hub connections joined through lateral extrusion, Applications in Engineering Science 6 (2021) 100047.
DOI: https://doi.org/10.1016/j.apples.2021.100047

[11] K.W. Chase, C.D. Sorensen B.J.K. DeCaires, Variation analysis of tooth engagement and loads in involute splines, IEEE Transactions on Automation Science and Engineering 7/4 (2010) 746-754.
DOI: https://doi.org/10.1109/TASE.2009.2033033

[12] F. Dörr, M. Funk, M. Liewald, H. Binz, R. Köstlmeier, Influence of internal hub profile on joining process of shaft-hub connection by lateral extrusion, Procedia Engineering 81 (2014) 1988-1993.
DOI: https://doi.org/10.1016/j.proeng.2014.10.269

[13] M. Funk, Load-bearing capacity of shaft-hub connections produced by means of transverse extrusion under torsional stress, PhD Thesis, University of Stuttgart, 2017 (in German).
DOI: https://doi.org/10.18419/opus-9366

[14] J. Żmudzki, G. Chladek, P. Malara, L.A. Dobrzański, M. Zorychta, K. Basa, The simulation of mastication efficiency of the mucous-borne complete dentures, Archives of Materials Science and Engineering 63/2 (2013) 75-86.

[15] J. Bimbo, S. Luo, K. Althoefer, H. Liu, In-hand object pose estimation using covariance-based tactile to geometry matching, IEEE Robotics and Automation Letters 1/1 (2016) 570-577.
DOI: https://doi.org/10.1109/lra.2016.2517244

[16] S. Medina, A.V. Olver, An analysis of misaligned spline coupling, Proceedings of the Institution of Mechanical Engineers, Part J: Journal of Engineering Tribology 216/5 (2002) 269-278.
DOI: https://doi.org/10.1243/135065002760364813

[17] F. Curà, A. Mura, F. Adamo, Fatigue damage in spline couplings: numerical simulations and experimental validation, Procedia Structural Integrity 5 (2017) 1326-1333.
DOI: https://doi.org/10.1016/j.prostr.2017.07.141

[18] J. Mucha, Finite element modeling and simulating of thermomechanic stress in thermocompression bondings, Materials and Design 30/4 (2009) 1174-1182. DOI: https://doi.org/10.1016/j.matdes.2008.06.026

[19] D.G. Pardhi, S.D. Khamankar, Stress analysis of spline shaft using finite element method and its experimental verification by photo elasticity, International Journal of Mechanical Engineering and Robotics Research 3/4 (2014) 451-458.

[20] G. Chladek, K. Basa, J. Żmudzki, P. Malara, A. Nowak, J. Kasperski, Influence of aging solutions on wear resistance and hardness of selected resin-based dental composites, Acta of Bioengineering and Biomechanics 18/3 (2016) 43-52. DOI: https://doi.org/10.5277/ABB-00434-2015-03

[21] G. Chladek, J. Żmudzki, P. Malara, L.A. Dobrzański, C. Krawczyk, Influence of introducing silver nanoparticles on tribological characteristics of soft liner, Archives of Materials Science and Engineering 62/1 (2013) 5-14.

[22] J. Żmudzki, G. Chladek, P. Malara, Use of finite element analysis for the assessment of biomechanical factors related to pain sensation beneath complete dentures during mastication, The Journal of Prosthetic Dentistry 120/6 (2018) 934-941.
DOI: https://doi.org/10.1016/j.prosdent.2018.02.002

[23] M. Czerwiński, J. Żmudzki, K. Kwieciński, M. Kowalczyk, Finite element analysis of the impact of the properties of dental wedge materials on functional features, Archives of Materials Science and Engineering 112/1 (2021) 32-41.
DOI: https://doi.org/10.5604/01.3001.0015.5930